

# Genome-wide identification of novel genetic markers from RNA sequencing assembly of diverse *Aegilops tauschii* accessions

Ryo Nishijima<sup>1</sup> · Kentaro Yoshida<sup>1</sup> · Yuka Motoi<sup>2</sup> · Kazuhiro Sato<sup>2</sup> · Shigeo Takumi<sup>1</sup>

Received: 20 March 2016 / Accepted: 21 April 2016 / Published online: 3 May 2016  
© Springer-Verlag Berlin Heidelberg 2016

**Abstract** The wild species in the Triticeae tribe are tremendous resources for crop breeding due to their abundant natural variation. However, their huge and highly repetitive genomes have hindered the establishment of physical maps and the completeness of their genome sequences. To develop molecular markers for the efficient utilization of their valuable traits while avoiding their genome complexity, we assembled RNA sequences of ten representative accessions of *Aegilops tauschii*, the progenitor of the wheat D genome, and estimated single nucleotide polymorphisms (SNPs) and insertions/deletions (indels). The deduced unigenes were anchored to the chromosomes of *Ae. tauschii* and barley. The SNPs and indels in the anchored unigenes, covering entire chromosomes, were sufficient for linkage map construction, even in combinations between the genetically closest accessions. Interestingly, the resolution of SNP and indel distribution on barley chromosomes was slightly higher than on *Ae. tauschii* chromosomes. Since barley chromosomes are regarded as virtual chromosomes of Triticeae species, our strategy allows capture of genetic markers arranged on the chromosomes in order based on

the conserved synteny. The resolution of these genetic markers will be comparable to that of the *Ae. tauschii* whose draft genome sequence is available. Our procedure should be applicable to marker development for Triticeae species, which have no draft sequences available.

**Keywords** *Aegilops tauschii* · DNA markers · *Hordeum vulgare* · RNA sequencing · Synteny

## Introduction

The tribe Triticeae includes many economically valuable cereals (e.g., barley, rye, and wheat) and their wild relatives. *Aegilops tauschii* Coss., the D-genome donor of bread wheat (*Triticum aestivum* L.), has been utilized for breeding wheat as a donor of important agricultural traits such as abiotic and biotic stress resistance (Matsuoka et al. 2013, 2015; Yang et al. 2014; Sehgal et al. 2015). The wild related species provide morphologically and genetically high diversity, acting as resources for potentially useful variability for cereal breeding. To accelerate introduction of these traits to crop species, it is necessary to develop efficient methods to find genetic markers linking the traits. However, the genome size of the Triticeae species is too large to develop high-quality physical maps, and whole genome sequencing of these species is still challenging.

Barley (*Hordeum vulgare* L.) provides one of the highest-quality genome sequences in the Triticeae. A high-resolution physical map and over 20,000 full-length cDNAs have also been released (Matsumoto et al. 2011; The International Barley Genome Sequencing Consortium, IBSC 2012). Barley is evolutionarily closer to wheat and its wild species than are other monocot species with high-quality genome sequences. Barley and wheat ancestors diverged

---

Communicated by S. Hohmann.

**Electronic supplementary material** The online version of this article (doi:10.1007/s00438-016-1211-2) contains supplementary material, which is available to authorized users.

---

✉ Kentaro Yoshida  
kentaro.yoshida@port.kobe-u.ac.jp

<sup>1</sup> Laboratory of Plant Genetics, Graduate School of Agricultural Science, Kobe University, Rokkodai 1-1, Nada, Kobe, Japan

<sup>2</sup> Institute of Plant Science and Resources, Okayama University, Kurashiki, Japan

13 million years ago (Gaut 2002). Chromosomal synteny of gene location is highly conserved between barley and wheat (Mayer et al. 2011; Wicker et al. 2011). Using this conserved synteny, genetic markers linked to phenotypes have been isolated. For example, Nishijima et al. (2014) found tightly linked markers of the *Iw2* locus of *Ae. tauschii*, which encodes a cuticular wax inhibitor and provides an evolutionary clue for the establishment of bread wheat. The D-genome donor of bread wheat is assumed to have been *Ae. tauschii* accessions with a recessive *iw2* allele, the habitat of which is limited to the area roughly from Transcaucasia to the southern coastal region of the Caspian Sea (Tsunewaki et al. 1966; Nishijima et al. 2014). Although the genome sequence of *Ae. tauschii* is available (Jia et al. 2013), many contigs have failed to be connected to chromosomal positions. A physical map of *Ae. tauschii* was constructed as well using more than 400,000 bacterial artificial chromosomes (Luo et al. 2013), but not all the sequences are accessible, preventing identification of tightly linked markers. To solve these problems, several SNP markers derived from RNA sequencing analyses (Iehisa et al. 2012, 2014) were assigned to the *Iw2* region, and the *Ae. tauschii* genome contigs that carry these markers were selected. Based on the synteny between barley and *Ae. tauschii*, additional contigs were assigned near the marker-carrying contigs, and the sequences of these additional contigs were searched for simple sequence repeat (SSR) motifs (Nishijima et al. 2014).

Designing useful SSR markers is laborious. Commonly, SSR markers are built based on repeats in the genome sequence and tested to determine whether these markers can detect variations in recombinant populations. To avoid this arduous process, a systematic way of designing genetic markers is needed. Whole genome sequencing of multiple samples from wild Triticeae species is not necessarily a convenient approach due to their large genome and the costs of sequencing. RNA sequencing will be a powerful approach to solve these problems. Here are some of its advantages: (1) it is applicable to species that have large and complex genomes, as it excludes intergenic repetitive regions, (2) it allows mapping of detected polymorphisms to chromosomes based on conserved coding regions and synteny between other grass species that have high-quality genome sequences, such as barley, rice, and *Brachypodium distachyon*, and (3) it can be used to measure gene expression level as well.

Iehisa et al. (2014) performed RNA sequencing from leaf and young spike tissues of two *Ae. tauschii* accessions using the 454 Life Sciences pyrosequencer and identified 13,347 high-confidence SNPs. The short reads were aligned to de novo assembled transcripts to call SNPs, and the assembled transcripts were mapped to the barley

genome. At that time, barley full-length cDNA information was unavailable. The comparisons between two accessions provided a limited number of genetic markers for the *Ae. tauschii* population (Iehisa et al. 2014). The Triticeae can be treated as a single genetic system, sharing homoeologous chromosomes (Mayer et al. 2011; Wicker et al. 2011), and the highly conserved synteny among the Triticeae species enables conducting genetic analyses of wild Triticeae species whose genome sequences are unavailable.

Here, we performed RNA sequencing of ten accessions of *Ae. tauschii* on the Illumina MiSeq platform to develop molecular markers. Through the RNA sequencing assembly, a large number of SNPs was found between accessions, even within the same lineages. The SNPs and indels were anchored to the chromosomes of *Ae. tauschii* and barley, and were distributed over the entire chromosomes. Using this approach, a large number of genetic markers can be efficiently obtained in Triticeae species even if the reference genome is incomplete.

## Materials and methods

### Plant materials, library construction and RNA sequencing

Based on population structure analyses, *Ae. tauschii* can be divided into two major lineages L1 and L2 (Table 1) (Mizuno et al. 2010; Matsuoka et al. 2013). *Ae. tauschii* that has given rise to the establishment of common wheat is presumed to belong to L2 (Mizuno et al. 2010; Matsuoka et al. 2013; Nishijima et al. 2014). The large part of the gene pool of *Ae. tauschii* remains unexplored for wheat breeding, especially in L1. The ten accessions of *Ae. tauschii* used were chosen as representative of the two major lineages, L1 and L2 (Table 1). Total RNA was extracted from leaves at the seedling stage using a Plant Total RNA Extraction Miniprep System (Viogene, Taipei Hsien, Taiwan, ROC). A total of 4 µg of RNA was used for constructing paired-end libraries following the manufacturer's instructions. The libraries were sequenced for 300 cycles × 2 on an Illumina MiSeq sequencer with 300-bp paired-end reads. Sequencing data have been deposited to DDBJ BioProject PRJDB4683.

### De novo assembly of short reads from RNA sequencing

Quality control of short reads was performed using the FastQC tool of the Galaxy portal (Giardine et al. 2005; Blankenberg et al. 2010; Goecks et al. 2010). Low-quality bases (average Phred quality score per 4 bp < 30), adapter sequences and reads <100 bp were removed using

**Table 1** *Ae. tauschii* accessions used in this study

Accession number	Origins	Lineage <sup>a</sup>	References	Resources
AT76	China	L1 (TauL1b)	Matsuoka et al. (2015)	Okayama University
PI499262	China	L1 (TauL1b)	Matsuoka et al. (2015)	United States Department of Agriculture
KU-2627	Afghanistan	L1-S1 (TauL1b)	Mizuno et al. (2010) Matsuoka et al. (2015)	Plant Germ-plasm Institute, Kyoto University
KU-2025	Afghanistan	L1-S2 (TauL1b)	Mizuno et al. (2010) Matsuoka et al. (2015)	Plant Germ-plasm Institute, Kyoto University
KU-2087	Iran	L1-S3 (TauL1b)	Mizuno et al. (2010) Matsuoka et al. (2015)	Plant Germ-plasm Institute, Kyoto University
KU-2003	Pakistan	L1-S4 (TauL1b)	Mizuno et al. (2010) Matsuoka et al. (2015)	Plant Germ-plasm Institute, Kyoto University
KU-2078	Iran	L2-S1 (TauL2x)	Mizuno et al. (2010) Matsuoka et al. (2015)	Plant Germ-plasm Institute, Kyoto University
KU-2124	Iran	L2-S1 (TauL2x)	Mizuno et al. (2010) Matsuoka et al. (2015)	Plant Germ-plasm Institute, Kyoto University
KU-2075	Iran	L2-S3 (TauL2x)	Mizuno et al. (2010) Matsuoka et al. (2015)	Plant Germ-plasm Institute, Kyoto University
KU-2093	Iran	L2-S3 (TauL2b)	Mizuno et al. (2010) Matsuoka et al. (2015)	Plant Germ-plasm Institute, Kyoto University

<sup>a</sup> The lineage name in the parenthesis is described in Matsuoka et al. (2015)

the Trimmomatic version 0.32 tool (Bolger et al. 2014). After filtering, paired short reads were merged into single reads based on overlapping regions using PEAR version 0.9.7 software (Zhang et al. 2014). The merged reads were assembled de novo using Trinity version 2.1.1 software (Grabherr et al. 2011; Haas et al. 2013) to reconstruct transcripts for each accession of *Ae. tauschii*. Trinity generates a fasta file, in which each nucleotide sequence harbors a header with an isoform number (e.g., i1 = isoform #1, i2 = isoform #2, etc.). If a gene had multiple isoforms, the transcript sequence of isoform #1 was picked up from the fasta file to construct a set of unigenes. The assembled transcripts have been deposited to Transcriptome Shotgun Assembly (TSA) division of DDBJ BioProject PRJDB4683.

### Mapping the assembled transcripts to *Ae. tauschii* and barley genome sequences

The representative transcripts were mapped to the *Ae. tauschii* reference genome “v1.25 masked” (Jia et al. 2013) and barley reference genome “v1.26 masked” (IBSC 2012) in Ensembl Plants (Kersey et al. 2015) using Gmap version 2013-03-31 software (Wu and Watanabe 2005; Quinlan and Hall 2010). For mapping to scaffolds of the *Ae. tauschii* genome, if the identity in the aligned region was >95 % and the coverage of the aligned region per total length of a transcript was >90 %, the transcript was regarded as mapping to a scaffold of *Ae. tauschii*. For mapping to the barley genome, if the identity was >78 % and the coverage was

>77 %, the transcript was regarded as mapping to a barley chromosome.

### Quantification of gene expression and identification of SNPs and indels between tested accessions

The merged reads of each *Ae. tauschii* accession were aligned pairwise to their corresponding unigenes using the Bowtie2 tool (Langmead and Salzberg 2012) with local alignment, generating 10 × 10 alignment outputs. We estimated depth of coverage over a transcript using SAMtools software with the command “samtools idxstats” (Li et al. 2009) and calculated counts per million (CPM) as a measure of gene expression level. Correlation coefficients for the CPM of each transcript between accessions were calculated using R software.

SNPs and indels were called from the alignment outputs using SAMtools and Coval software with the option “-freq 0.95 -m 1000000 -n 10” (Kosugi et al. 2013). SNP calling with Coval is successful in identification of causal SNPs and genetic markers linked to phenotypes (Abe et al. 2012; Takagi et al. 2013). To acquire novel SNP markers between the *Ae. tauschii* accessions, we chose only homozygous SNPs and indels, because *Ae. tauschii* is a self-fertilizing species. Anchoring of SNPs and indels to the scaffolds of *Ae. tauschii* and barley chromosomes was performed based on the outputs of Gmap for mapping unigenes to these scaffolds and chromosomes. To link the scaffolds of *Ae. tauschii* to the genetic map of *Ae. tauschii* (Luo et al. 2013), the positional information from

Supplementary Material 4 in Iehisa et al. (2014) was used. All SNP information is available from our laboratory web site (<http://www.lab.kobe-u.ac.jp/ans-plantgenetics/index.html>).

### Marker construction and genotyping

To assess the usefulness of the SNP library, cleaved amplified polymorphic sequence (CAPS) or derived CAPS markers were developed to the chromosomal region around *Iw2*, a dominant non-glaucous allele, on the short arm of chromosome 2D. In our previous study, some *Ae. tauschii* scaffolds were anchored to this region (Nishijima et al. 2014). SNPs mapping to these scaffolds in silico were used to develop molecular markers. The primer sequences for each SNP marker and relevant restriction enzymes are summarized in Supplementary Table S1. PCR and subsequent analyses were performed as described previously (Iehisa et al. 2012, 2014).

### SNP assignment and association analysis

In Nishijima et al. (2014), we developed a genetic map of *Iw2* using  $F_2$  mapping population derived from a cross between KU-2003 (L1 lineage and non-glaucous phenotype) and KU-2124 (L2 lineage and glaucous phenotype). Newly generated SNP markers through the RNA sequencing analysis were assigned to this framework. Another 210 *Ae. tauschii* accessions (Takumi et al. 2011; Nishijima et al. 2014) were also genotyped using these markers to assess the genetic associations among the markers and glaucous phenotype. Association was analyzed using a mixed linear model function in TASSEL ver. 5.0 software (Bradbury et al. 2007). The  $Q$  matrix of population membership probabilities was derived from population structure analysis of *Ae. tauschii* accessions and kinship was calculated in TASSEL based on the genotyping information of the 169 DArT markers for the 206 *Ae. tauschii* accessions (Matsuoka et al. 2013).

## Results

### Reconstruction of transcript sequences of the ten accessions of *Aegilops tauschii*

To obtain novel genetic markers for the D genome, we performed RNA sequencing of the ten accessions of *Ae. tauschii* (Table 1). To cover the entire genetic variation of *Ae. tauschii*, we chose representative accessions from both lineages I (L1) and II (L2) including sublineages (Mizuno et al. 2010; Matsuoka et al. 2013, 2015). Altogether, 4.8–5.8 million paired-end short reads were obtained for each accession (Supplementary Table S2) and analyzed

according to the workflow shown in Fig. 1. After filtering and merging of these short reads, 2.6–3.6 million high-quality reads were acquired. The average length of the merged reads was about 327 bp. After de novo assembly of the merged reads, 33,680–65,827 transcripts were reconstructed for each accession, with N50 values of 1369–1519 bp. If a transcript had more than one isoform, one of the isoforms from the transcript was selected as a unigene. Finally, a set of unigenes for each accession, containing 29,386–55,268 representative isoforms, was obtained (Supplementary Table S3).

To evaluate how many unigenes link to the published genome sequences of *Ae. tauschii* (Jia et al. 2013) and barley (IBSC 2012), the unigene sequences for each accession were aligned to these genome sequences. Of the total unigenes, 65.7–79.7 % were mapped to *Ae. tauschii* and 29.8–39.1 % to barley genome sequences (Supplementary Table S3). As expected, the number of unigenes that mapped to *Ae. tauschii* sequences was higher than to barley sequences. Only a few percent of the unigenes specifically mapped to the barley sequences. The unigenes unmapped to both genome sequences occupied 15.6–29.8 % of the total and could have been derived from accession-specific genomic regions or could be due to the incompleteness of the reference genome.

In order to compare nucleotide sequences of transcripts between *Ae. tauschii* accessions, plants were grown under the same conditions and their leaves were sampled at the same stage. To assess the pattern of gene expression in these samples, we estimated CPM, a commonly used parameter of gene expression, and calculated the correlation coefficient of CPM between all the possible pairs of the ten accessions (Supplementary Table S4). All the pairwise comparisons showed significant positive correlations, indicating that there was no drastic difference in gene expression between the tested samples.

### Detection of nucleotide polymorphisms in *Ae. tauschii*

To estimate how many potential genetic markers between accessions could be constructed, we counted SNPs and indels from the pairwise comparisons according to the thresholds with read depth  $>3$  (Supplementary Table S5) or  $>10$  (Table 2). More SNPs and indels were found under the thresholds with read depth  $>3$ . Although the set of SNPs and indels with read depth  $>3$  may include some false positives, it may be useful in searching for genetic markers to use for genetic linkage analysis when no marker candidates are available in the set with read depth  $>10$ . Here, we conducted downstream analyses using the set of high-confidence SNPs and indels with read depth  $>10$ .

The number of SNPs and indels between accessions is dependent on comparisons between and within lineages

**Fig. 1** The RNA sequencing analysis workflow for constructing genetic markers of *Ae. tauschii*

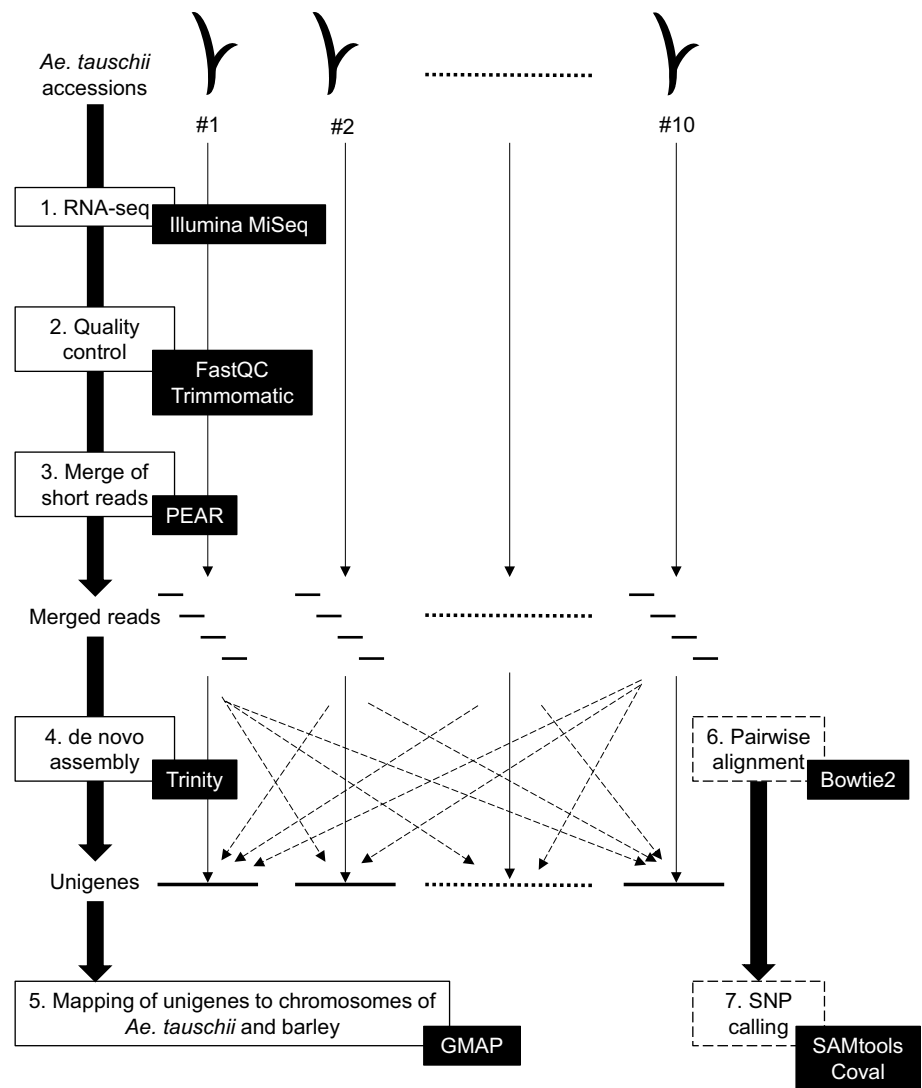


(Table 2). In pairwise comparisons between the same accessions, 98–1492 SNPs and 4–20 indels were detected. These SNPs and indels could be false positives generated by nucleotide differences between paralogous genes in the same genome. The average number of SNPs between lineages L1 and L2 was 37,408 and the average number of indels was 2041. Within L1, the average number of SNPs and indels was 16,778 and 919, respectively. Within L2, the average number of SNPs and indels was 22,875 and 951, respectively. Even within the lineages, a large number of potential genetic markers was obtained.

Nucleotide differences of 3 bp between PCR amplicons can be detected by 6 % polyacrylamide gel electrophoresis. The estimated indels >3 bp can be directly used as co-dominant markers. To evaluate how many indels are available for development of co-dominant markers, the distribution of the length of indels was examined (Supplementary Fig. S1). The average number of indels >3 bp was 863, 378, and 411, respectively, between the lineages, within L1,

and within L2. These indels can be used for initial rough mapping.

Transcript expression levels may affect SNP and indel frequencies per transcript. To evaluate the impact of gene expression on the SNP and indel frequencies, the correlation between CPM and the number of polymorphisms per transcript was calculated (Supplementary Fig. S2). No clear correlation was found between CPM and the number of polymorphisms, indicating that the gene expression levels did not influence the SNP and indel frequencies under our criteria for SNP and indel calling.

#### Anchoring SNPs and indels to scaffolds and chromosomes of *Ae. tauschii*

To develop genetic markers anchored to the chromosomes of *Ae. tauschii*, we evaluated how many SNPs and indels were anchored to scaffolds of the draft genome or the chromosomes of *Ae. tauschii* (Table 3, Supplementary Table

**Table 2** The number of SNPs and indels detected in each transcript-read pairing of ten *Ae. tauschii* accessions (depth >10)

	Transcript model	Read										
		L1					L2					
		AT76	PI499262	KU-2627	KU-2025	KU-2087	KU-2003	KU-2078	KU-2124	KU-2075	KU-2093	
L1	AT76	168	24464	8316	13833	9587	7557	42153	45080	46808	42747	SNP
		13	1368	472	708	555	460	2416	2533	2599	2240	Indel
	PI499262	21329	197	32872	12153	34614	28832	19012	30089	26789	25091	SNP
		1134	8	1745	645	1934	1604	1085	1623	1426	1321	Indel
	KU-2627	5931	25121	302	13784	10401	7309	45772	47993	50528	45253	SNP
		292	1376	11	694	559	379	2616	2591	2806	2349	Indel
	KU-2025	20568	19143	29150	98	30951	25330	24902	30063	27436	24284	SNP
		1134	1095	1639	5	1719	1398	1381	1668	1422	1266	Indel
	KU-2087	6346	25201	9809	14329	266	7694	45567	47877	49400	45017	SNP
		351	1483	500	721	4	420	2642	2687	2765	2325	Indel
KU-2003	6015	20896	8399	13633	10075	252	45566	45534	49792	44860	SNP	
	321	1222	409	691	548	10	2610	2586	2763	2328	Indel	
L2	KU-2078	31924	15026	50912	13480	52313	44929	361	20051	13708	13695	SNP
		1720	825	2671	685	2891	2438	15	1179	760	769	Indel
	KU-2124	78154	55971	103752	42438	103756	97379	43454	1492	45698	42744	SNP
		1742	1315	2837	807	2879	2489	1125	20	1238	1042	Indel
	KU-2075	31982	19685	51144	13617	50412	42150	12457	19518	377	13717	SNP
		1689	1096	2724	645	2766	2320	707	1119	14	733	Indel
	KU-2093	31684	21461	50642	13019	52124	44159	13723	20082	15656	349	SNP
		1732	1192	2667	667	2793	2327	784	1115	842	14	Indel

S6). Of the total SNPs in the pairwise comparisons, an average of 68.5 and 17.8 % were, respectively, anchored to the scaffolds and chromosomes. There was no large difference in the percentage of SNPs mapping to the scaffolds (61.0–79.8 %) or the chromosomes (10.8–21.9 %) for any pairwise comparisons. The number of these anchored SNPs was directly proportional to the total number of SNPs (Tables 2, 3). Unfortunately, 78.1–89.2 % of SNPs remained unmapped to the chromosomes, even when the SNPs and indels were anchored to the scaffolds. Indels showed the same tendency as the SNPs (Table 2, Supplementary Table S6). Although the scaffolds cover 84.3 % of the *Ae. tauschii* genome (4.23-Gb), only 1.72-Gb is anchored to the chromosomes (Jia et al. 2013). Thus, the number of SNPs and indels mapped to the chromosomes were limited as well.

The average number of SNPs per chromosome within L1, within L2 and between L1 and L2 was 312.2–678.0, 209.3–413.0 and 816.2–1356.8, respectively (Supplementary Table S7). Except for chromosome 7, a large coefficient of variation in the number of SNPs within L1 (0.66–0.83) was detected (Supplementary Fig. S3; Table S7). The number of SNPs for some pairwise comparisons within L1 was greater than between L1 and L2

on six chromosomes. The average number of SNPs on chromosome 6D was smaller than on the other chromosomes, but no clear differences were found among the chromosomes when the average number of SNPs per transcript was estimated. The same tendency was detected for the indels (Supplementary Fig. S3; Table S8).

To develop molecular markers for genetic linkage analysis, uniform distribution of SNPs and indels over the chromosomes is desirable. The distributions of transcripts, SNPs and indels over the seven chromosomes were visualized in representative pairs within L1 (Fig. 2a), within L2 (Fig. 2b), and between L1 and L2 (Fig. 2c). These representative pairs represent the most and least SNP- and indel-rich pairs in each combination of lineages. Although the SNPs were not evenly distributed, they covered all chromosomes moderately well in intra- and interlineage comparisons. Compared with the SNPs, indels were more unevenly distributed. At least a small number of indels was located on each chromosome. A high density of SNPs and indels was detected around the centromeric regions. This observation could be explained by the suppression of recombination in these regions, generating gaps between physical and genetic distance.

**Table 3** The number of SNPs mapped to the draft genome or the chromosomes of *Ae. tauschii* out of the SNPs detected in each transcript-read pairing of ten *Ae. tauschii* accessions

Transcript model	Read	Read										Mapped to
		L1					L2					
		AT76	PI499262	KU-2627	KU-2025	KU-2087	KU-2003	KU-2078	KU-2124	KU-2075	KU-2093	
L1	AT76	92	18038	5737	9752	6539	5266	30950	33317	34510	31281	Genome
			(73.7)	(69.0)	(70.5)	(68.2)	(69.7)	(73.4)	(73.9)	(73.7)	(73.2)	
		20	5081	1295	2653	1509	1168	8501	8949	9337	8238	Chr.
			(20.8)	(15.6)	(19.2)	(15.7)	(15.5)	(20.2)	(19.9)	(19.9)	(19.3)	
	PI499262	16213	99	25445	8717	26677	22525	13114	21414	19050	17603	Genome
		(76.0)		(77.4)	(71.7)	(77.1)	(78.1)	(69.0)	(71.2)	(71.1)	(70.2)	
		4333	19	6813	2186	7246	6121	3251	4917	4380	4152	Chr.
		(20.3)		(20.7)	(18.0)	(20.9)	(21.2)	(17.1)	(16.3)	(16.3)	(16.5)	
	KU-2627	3689	18304	123	9644	6519	4859	32454	33945	35754	31748	Genome
		(62.2)	(72.9)		(70.0)	(62.7)	(66.5)	(70.9)	(70.7)	(70.8)	(70.2)	
		954	5166	26	2848	1589	1090	8502	8896	9552	8256	Chr.
		(16.1)	(20.6)		(20.7)	(15.3)	(14.9)	(18.6)	(18.5)	(18.9)	(18.2)	
KU-2025	16194	14706	22959	51	24248	20201	18652	22460	20519	18123	Genome	
	(78.7)	(76.8)	(78.8)		(78.3)	(79.8)	(74.9)	(74.7)	(74.8)	(74.6)		
	4345	3673	6347	4	6590	5555	4697	5113	4924	4386	Chr.	
	(21.1)	(19.2)	(21.8)		(21.3)	(21.9)	(18.9)	(17.0)	(17.9)	(18.1)		
KU-2087	4065	18414	6743	10026	162	5245	32657	34034	35543	32151	Genome	
	(64.1)	(73.1)	(68.7)	(70.0)		(68.2)	(71.7)	(71.1)	(71.9)	(71.4)		
	823	5156	1398	2705	35	1144	8816	9021	9548	8401	Chr.	
	(13.0)	(20.5)	(14.3)	(18.9)		(14.9)	(19.3)	(18.8)	(19.3)	(18.7)		
KU-2003	3911	15211	5512	9664	6142	128	32339	32215	35381	31713	Genome	
	(65.0)	(72.8)	(65.6)	(70.9)	(61.0)		(71.0)	(70.7)	(71.1)	(70.7)		
	727	4099	1170	2601	1316	18	8581	8414	9655	8335	Chr.	
	(12.1)	(19.6)	(13.9)	(19.1)	(13.1)		(18.8)	(18.5)	(19.4)	(18.6)		
L2	KU-2078	23977	11430	39109	9868	40000	34827	190	13954	9774	9785	Genome
		(75.1)	(76.1)	(76.8)	(73.2)	(76.5)	(77.5)		(69.6)	(71.3)	(71.4)	
		6563	2963	10525	2601	10769	9419	46	2644	1673	1867	Chr.
		(20.6)	(19.7)	(20.7)	(19.3)	(20.6)	(21.0)		(13.2)	(12.2)	(13.6)	
	KU-2124	24152	17904	40666	11533	40148	34639	14150	160	15715	13853	Genome
		(77.2)	(76.4)	(78.6)	(76.1)	(77.6)	(78.8)	(75.0)		(75.0)	(74.7)	
		6275	4202	10381	2661	10396	9017	2495	20	2857	2525	Chr.
		(20.1)	(17.9)	(20.1)	(17.6)	(20.1)	(20.5)	(13.2)		(13.6)	(13.6)	
	KU-2075	24038	14415	39009	10043	38176	32300	8474	13363	185	9275	Genome
		(75.2)	(73.2)	(76.3)	(73.8)	(75.7)	(76.6)	(68.0)	(68.5)		(67.6)	
		6341	3330	10312	2456	10384	8688	1349	2405	26	1642	Chr.
		(19.8)	(16.9)	(20.2)	(18.0)	(20.6)	(20.6)	(10.8)	(12.3)		(12.0)	
KU-2093	24338	16116	39131	9660	40055	34545	9904	14177	11252	147	Genome	
	(76.8)	(75.1)	(77.3)	(74.2)	(76.8)	(78.2)	(72.2)	(70.6)	(71.9)			
	6381	3858	10136	2324	10413	9111	1753	2545	1898	37	Chr.	
	(20.1)	(18.0)	(20.0)	(17.9)	(20.0)	(20.6)	(12.8)	(12.7)	(12.1)			

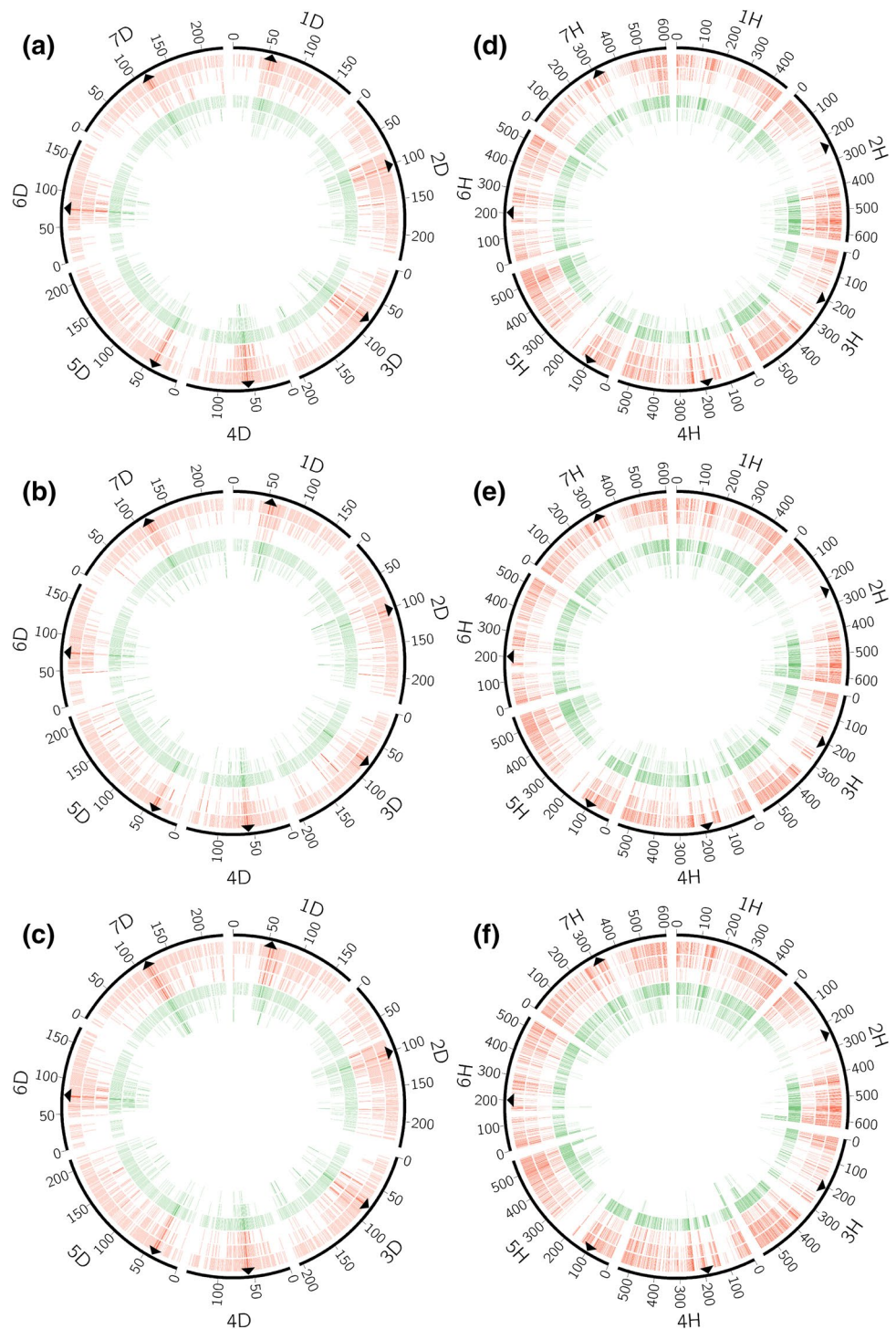
The number in parenthesis shows the proportion (%) of the mapped SNPs to all SNPs in Table 2

### Anchoring SNPs and indels to the chromosomal pseudomolecules of barley

To evaluate whether the barley physical map is useful for assigning SNPs and indels between *Ae. tauschii* accessions in the same order on their chromosomes, the

estimated SNPs and indels were mapped to the barley chromosomes (Table 4, Supplementary Table S9). An average of 29.1 % of the total SNPs and 25.4 % of the indels were anchored to the barley chromosomes. The percentages of anchored SNPs and indels were almost the same in any pairwise comparison. Interestingly, the

**Fig. 2** Distribution of SNPs and indels detected in pairwise comparison of *Ae. tauschii* accessions on the genetic map of *Ae. tauschii* (a–c, scale in cM) and the physical map of barley (d–f scale in Mb). Three circles of the same color show the number of transcripts, SNPs, and indels from the outer to inner circles. The red circles represent the richest SNP and indel pairs, and the green circles, the least rich pairs in each combination of lineages: **a** L1 vs L1, KU-2087 read-mapped to PI499262 transcript and AT76 to KU-2003, **b** L2 vs L2, KU-2093 to KU-2124 and KU-2078 to KU-2075, **c** L1 vs L2, KU-2087 to KU-2078 and KU-2025 to KU-2093, **d** L1 vs L1, KU-2087 to PI499262 and AT76 to KU-2627, **e** L2 vs L2, KU-2075 to KU-2124 and KU-2078 to KU-2075, and **f** L1 vs L2, KU-2075 to AT76 and PI499262 to KU-2078. Arrowheads indicate centromeric positions of each chromosome, except for chromosome 1H, which only had whole-chromosome sequence (IBSC 2012)



number of SNPs and indels anchored to the barley chromosomes was larger than the number anchored to the chromosomes of *Ae. tauschii* in all pairwise comparisons (Tables 3, 4).

The average number of SNPs per chromosome within L1, within L2, and between L1 and L2 was 413.4–929.4, 481.6–851.5, and 1306.4–1849.0, respectively

(Supplementary Table S10). The average number of indels per chromosome within L1, within L2, and between L1 and L2 was 18.9–46.0, 22.9–43.7, and 67.4–89.9, respectively (Supplementary Table S11). These numbers were larger than for those anchored to the *Ae. tauschii* chromosomes. A similar observation was detected in the average number of SNPs and indels per transcript on each chromosome. As



**Table 4** The number of SNPs mapped to the barley physical map out of the SNPs detected in each transcript-read pairing of ten *Ae. tauschii* accessions

Transcript model	Read									
	L1					L2				
	AT76	PI499262	KU-2627	KU-2025	KU-2087	KU-2003	KU-2078	KU-2124	KU-2075	KU-2093
<b>L1</b>										
AT76	28 (32.9)	8042 (30.6)	2545 (29.2)	4043 (30.6)	2937 (33.1)	2499 (33.7)	14202 (33.2)	14948 (33.8)	15841 (33.6)	14356 (33.6)
PI499262	5907 (27.7)	44 (29.0)	9545 (28.8)	3496 (29.7)	10274 (30.2)	8719 (31.4)	5978 (29.5)	8874 (30.3)	8106 (29.8)	7486 (29.8)
KU-2627	1283 (21.6)	7019 (27.9)	83 (28.8)	3967 (24.8)	2583 (26.2)	1918 (29.1)	13315 (29.4)	14110 (29.0)	14642 (29.1)	13173 (29.1)
KU-2025	6357 (30.9)	6523 (34.1)	10264 (35.2)	53 (35.4)	10963 (35.4)	8979 (34.9)	8693 (34.0)	10216 (35.0)	9615 (34.9)	8467 (34.9)
KU-2087	1551 (24.4)	6921 (27.5)	2280 (23.2)	4099 (28.6)	40 (23.8)	1835 (28.6)	13027 (28.5)	13639 (28.7)	14177 (28.7)	12556 (27.9)
KU-2003	1521 (25.3)	6217 (29.8)	2003 (23.8)	4249 (31.2)	2570 (25.5)	68 (30.8)	14057 (29.7)	13536 (30.6)	15221 (30.6)	13634 (30.4)
<b>L2</b>										
KU-2078	8444 (26.5)	4428 (29.5)	14450 (28.4)	3550 (26.3)	15266 (29.2)	13135 (29.2)	76 (25.4)	5091 (26.1)	3574 (26.1)	3459 (25.3)
KU-2124	8831 (28.2)	6735 (28.8)	15310 (29.6)	4143 (27.3)	15487 (29.9)	12891 (29.3)	5081 (26.9)	132 (27.3)	5728 (27.3)	4968 (26.8)
KU-2075	8916 (27.9)	5704 (29.0)	14617 (28.6)	3725 (27.4)	14824 (29.4)	12522 (29.7)	3139 (25.2)	5269 (27.0)	91 (26.7)	3658 (26.7)
KU-2093	9176 (29.0)	6581 (30.7)	15069 (29.8)	3936 (30.2)	15699 (30.1)	13562 (30.7)	3602 (26.2)	5436 (27.1)	4022 (25.7)	101 (25.7)

The number in parenthesis shows the proportion (%) of the mapped SNPs to all SNPs in Table 2

observed for the SNPs anchored to the *Ae. tauschii* chromosomes, a large coefficient of variation in the number of SNPs (0.62–0.83) and indels (0.55–0.76) within L1 was detected, except for chromosome 7H (Supplementary Fig. S4; Tables S10, S11).

To determine whether the SNPs and indels that were anchored to the barley chromosomes were evenly distributed over the entire chromosomes, the distribution of these SNPs and indels was visualized. We chose pairs having the most or least numbers of SNPs and indels within L1 (Fig. 2d), within L2 (Fig. 2e), and within L1 and L2 (Fig. 2f). In all combinations excluding the pairs with the least number of SNPs between L1 and L2 (between PI499262 and KU-2078), SNPs covered the entire region of the chromosomes except for the unigene-sparse regions, one of which corresponded to the centromeric region of chromosome 2H. In the pairs with the least number of SNPs between L1 and L2 (between PI499262 and KU-2078), a high-density localization of SNPs was observed only for chromosomes 1H and 7H. Although the distribution of indels was not as uniform as that of SNPs, every chromosome carried a small number of indels in any comparison.

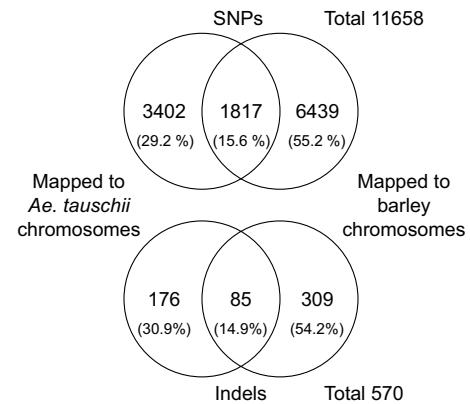


**Fig. 3** Venn diagrams of SNPs mapped to the *Ae. tauschii* and barley genomes. The numbers indicate mean values of SNPs and indels

### Integration of SNPs and indels that were anchored to the chromosomes of *Ae. tauschii* and barley

If the SNPs and indels anchored to *Ae. tauschii* chromosomes are different from those anchored to barley chromosomes, utilization of these SNPs and indels increases the

number of potential genetic markers. We tested overlaps between the SNPs and indels that were anchored to *Ae. tauschii* and barley chromosomes (Fig. 3). Venn diagrams of mean values of SNPs and indels showed that most SNPs and indels were specifically anchored to *Ae. tauschii* or barley chromosomes. Only 15.6 and 14.9 % of the total SNPs and indels overlapped. These results indicated that the integration of SNPs and indels anchored to the chromosomes of *Ae. tauschii* and barley increased the available genetic markers for linkage analysis.

### Application of CAPS markers to linkage and association analyses

To evaluate the usefulness of the SNP dataset, *Iw2* region specific markers were designed based on in silico mapping of transcript models to *Ae. tauschii* scaffolds. We developed 14 markers on 4 scaffolds (Supplementary Fig. S5). For ten markers, the genotyping results were consistent with the allelic type detected in RNA-seq. For the other four markers, however, genotypes of some accessions (*scaf43829\_1*, 2, and 7 for PI499262 and KU-2025 and *scaf10812\_2* for KU-2124) contradicted the results of RNA-seq. This observation suggests that the transcript models were constructed by reads derived from paralogues on other chromosomes. No specific PCR products were detected for a few SNP markers in several accessions, for which reads were absent at the SNP sites, e.g., *scaf10812\_6* for KU-2093, KU-2075, and KU-2078 and *scaf10812\_8* for six L1 accessions. This result indicated that some chromosomal rearrangements had occurred during divergence among the *Ae. tauschii* accessions, and that the genomic segments from which these markers were derived did not exist in the accessions that had no reads on the sites.

To confirm whether these markers were precisely linked to the *Iw2* locus on chromosome 2DS, we genotyped  $F_2$  individuals of the KU-2003/KU-2124 population using ten markers that were polymorphic between KU-2003 and KU-2124. Of the selected markers, seven mapped to the *Iw2* region and the remaining three markers were assigned to another chromosome (Fig. 4). The *Iw2* locus was mapped within a 0.9 cM interval between the most closely linked markers and co-localized with two markers. The chromosomal order of selected scaffolds at the *Iw2* region was consistent with that predicted in a previous study (Nishijima et al. 2014). Association analysis showed that five out of the seven markers that mapped to the *Iw2* region were significantly ( $P < 1E^{-3}$ ) associated with the glaucous/non-glaucous trait in *Ae. tauschii* (Table 5). All 20 glaucous accessions had the KU-2124-type allele at *scaf10812\_2* and *scaf10812\_6*, and most non-glaucous accessions had the KU-2003-type allele at *scaf43829\_9*. These results demonstrated that a fine map could be constructed efficiently

using SNPs derived from RNA-seq. Thus, the SNP dataset might be useful for molecular marker development in the specific chromosomal region of the D genome or across the entire genome.

## Discussion

### RNA sequencing as an efficient tool for SNP discovery and its potential for evolutionary studies in *Ae. tauschii*

We performed 300-bp paired-end RNA sequencing of leaf tissues from ten representative *Ae. tauschii* accessions including both the L1 and L2 lineages with the purpose of SNP identification and molecular marker development using the Illumina MiSeq platform. RNA sequencing of samples obtained from tissues grown under the same conditions generated a similar pattern of gene expression between the accessions, facilitating the detection of a large number of SNPs. The average number of SNPs between L1 and L2 (78,519) was four times higher than discovered in previous studies by transcriptome sequencing of leaves and spikes of two *Ae. tauschii* accessions, one each from L1 and L2 (Iehisa et al. 2012, 2014). Iehisa et al. (2014) performed RNA sequencing of leaf and spike tissues from the two *Ae. tauschii* accessions using 454 sequencing and detected 16,148 high-confidence SNPs. However, 300-bp paired-end sequencing on the MiSeq platform can generate long reads of higher quality. The length of the merged reads is comparable to the length of expressed sequence tags. This distinguishing characteristic enables detection of more SNPs, even from RNA sequencing data of only leaf tissue.

The increased number of SNPs among various accessions will help to construct more detailed genetic maps of the D genome. Although most intralinear pairings had fewer SNPs than interlinear pairings (Table 2), the least polymorphic pair had as many SNPs as the previous report (Iehisa et al. 2014). This result suggests that even intralinear crosses could possess enough polymorphisms for construction of genetic linkage maps. Molecular markers derived from the SNP dataset were actually assigned around the *Iw2* locus (Fig. 4), and were as densely distributed as our previous study (Nishijima et al. 2014), demonstrating that a fine map could be constructed efficiently using SNPs derived from RNA sequencing. This SNP dataset allows development of molecular markers in any specific chromosomal region of the D genome.

As expected, the number of indels was much smaller than that of SNPs. Since indels in exons often cause frame-shift mutations, purifying selection removes such deleterious mutations from the population. This is one of the disadvantages of marker development based on RNA

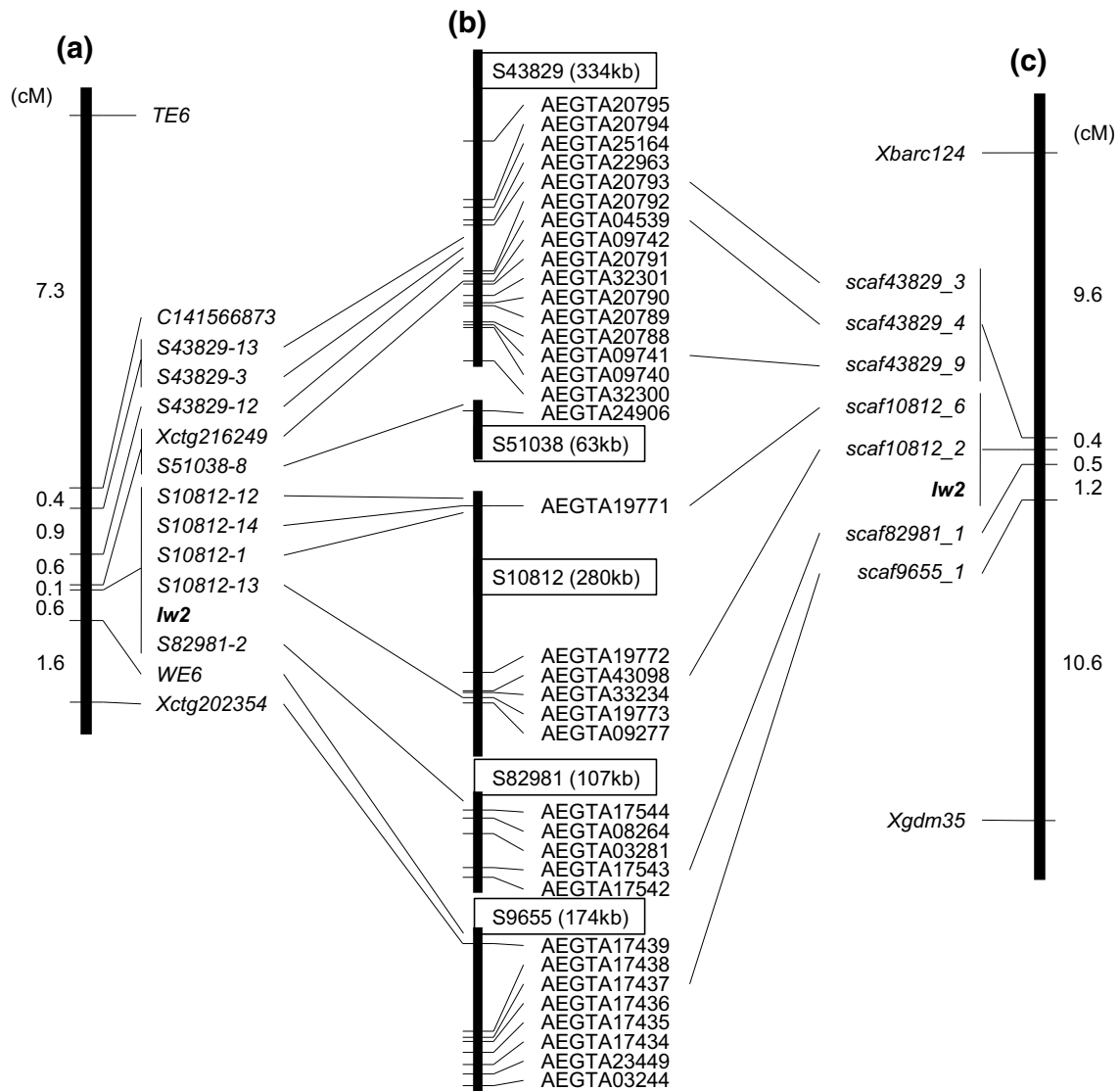


**Fig. 4** Comparison of linkage maps of the *Iw2* region. **a** Genetic map of the KU-2154/KU-2126  $F_2$  population (Nishijima et al. 2014). **b** The *Ae. tauschii* scaffolds anchored to the chromosomal region

(Nishijima et al. 2014). The positions of genes and markers on the two maps are indicated. **c** The linkage map constructed using markers developed in this study

sequencing. Indels, however, were detected across entire chromosomes as well (Fig. 2). The average number of indels that were anchored to the chromosomes was >10 on each chromosome in most of the pairwise comparisons of *Ae. tauschii* accessions. They should be useful for rough mappings, as PCR-based indel markers can be genotyped more easily than SNP markers.

Pairwise comparisons between the ten accessions of *Ae. tauschii* revealed a large variance in the number of SNPs and indels on chromosomes within L1 except for 7D, where some combinations between L1 and L2 accessions had a smaller number of SNPs and indels than between L1 accessions. These observations suggest the existence of gene flow between L1 and L2 lineages on these chromosomes,

whereas the number of SNPs on chromosome 7D between the L1 and L2 lineages was clearly larger than within L1 or within L2. The intraspecific lineage structure of *Ae. tauschii* is associated with differences in seed production and flowering time (Matsuoka et al. 2015). In particular, the L1 lineage with its high seed production and early flowering time has spread across East Asia (Matsuoka et al. 2015). The L1 lineage may have loci related to adaption to different habitats, preventing gene flow on chromosome 7D and generating a clear divergence between the L1 and L2 lineages.

The present study used only ten accessions, which are not enough to address evolutionary questions such as the above hypothesis. To dissect the evolutionary dynamics of

**Table 5** Genetic association between *Iw2*-linked marker genotypes and glaucous/non-glaucous phenotype in 210 accessions of *Ae. tauschii*

Marker name	Genotyped accession no.	Glaucous phenotype ( $N = 20$ ) <sup>a</sup>		Non-glaucous phenotype ( $N = 190$ ) <sup>a</sup>		Association analysis <sup>a</sup> <i>P</i> value
		KU-2003-type	KU-2124-type	KU-2003-type	KU-2124-type	
<i>scaf43829_3</i>	208	9	11	55	133	0.60281
<i>scaf43829_4</i>	197	9	11	174	3	4.47E–05
<i>scaf43829_9</i>	210	8	12	189	1	1.98E–11
<i>scaf10812_6</i>	186	0	20	142	24	1.48E–09
<i>scaf10812_2</i>	208	0	20	135	53	8.70E–06
<i>scaf82981_1</i>	209	1	19	148	41	1.36E–05
<i>scaf9655_1</i>	210	0	20	48	142	0.7121

The numbers of accessions for each genotype are represented in glaucous and non-glaucous phenotypes

<sup>a</sup> The phenotypes were evaluated in Nishijima et al. 2014

<sup>b</sup> The values were calculated based on a mixed linear model in the TASSEL ver. 5.0 software

the *Ae. tauschii* population, it is necessary to study nucleotide polymorphisms in more *Ae. tauschii* accessions. We found no clear correlations between gene expression level and SNP frequency per transcript (Fig. S2). This allowed SNPs identified through RNA sequencing to capture the genome-wide genetic diversity in the *Ae. tauschii* population without any bias derived from differences in gene expression level. Since the costs of RNA sequencing are fairly low owing to the development of next-generation sequencing technology and improvements in library construction (Townsend et al. 2015), the approach of RNA sequencing will make revealing genome-wide nucleotide polymorphisms in over a hundred samples of *Ae. tauschii* accessions feasible in the near future.

#### Advantages of RNA sequencing in the development of novel genetic markers for Triticeae

To reduce the complexity of genome sequencing, many derivatives of next-generation sequencing have been developed for the development of genetic markers (Kumar et al. 2012). In genotyping-by-sequencing and restriction site-associated DNA sequencing, restriction enzymes are used to create reduced representation libraries for sequencing (Davey et al. 2011). Although this method has been useful for SNP identification, the choice of enzymes might be a critical factor, and a portion of the sequenced reads such as repetitive elements might be discarded from the following analyses, especially in the Triticeae species, which have a large and complex genome. On the other hand, RNA sequencing focuses on exons only and fails to detect abundant polymorphisms in intragenic regions. SNPs between tested samples can be detected only in expressed genes. However, our study demonstrated that RNA sequencing

enables detection of a large number of SNPs, even between genetically close accessions of *Ae. tauschii*. In addition, our approach based on RNA sequencing assembly can make almost full use of the sequenced reads, and requires no prior information about the genome of interest. Based on the conserved gene order between barley and its crop relatives, SNPs can be anchored to specific chromosomal regions. From these points of view, RNA sequencing should be a reasonable approach for the development of molecular markers in the Triticeae.

The number of SNPs aligned to the *Ae. tauschii* genome was twice that of barley (Tables 3, 4). However, the number of SNPs mapping to chromosomes was slightly higher for barley (Tables 3, 4), consistent with a previous report (Iehisa et al. 2014), suggesting that molecular markers can be designed to specific target chromosomes using genomic information from barley as precisely as information from *Ae. tauschii*. These results also imply the versatility of the barley genome for the dissection of the genomes of other Triticeae species, since the synteny between barley and wheat relatives is widely conserved (Mayer et al. 2011; Wicker et al. 2011). In conclusion, our strategy, in which SNPs detected through RNA sequencing assembly are anchored to the seven chromosomes in silico based on the conserved synteny, can develop a large number of molecular markers and should be applicable to marker development for other wild species in the tribe Triticeae, at least diploids such as *Ae. caudata* (C genome), *Ae. umbellulata* (U genome) and *Ae. comosa* (M genome), which have no draft sequences available at all.

**Acknowledgments** Computations for the RNA sequencing assembly and alignments of short reads were performed on the NIG supercomputer at the ROIS National Institute of Genetics.

## Compliance with ethical standards

**Funding** This work was supported by a Grant from the Ministry of Education, Culture, Sports, Science and Technology of Japan [Grant-in-Aid for Scientific Research (B) Nos. 25292008 and 16H04862] to ST, and by MEXT as part of a Joint Research Program implemented at the Institute of Plant Science and Resources, Okayama University, Japan.

**Conflict of interest** The authors declare that they have no conflict of interest.

**Ethical standards** This article does not contain any studies with human participants or animals performed by any of the authors.

## References

- Abe A, Kosugi S, Yoshida K, Natsume S, Takagi H, Kanzaki H, Matsumura H, Yoshida K, Mitsuoka C, Tamiru M, Innan H, Cano L, Kamoun S, Terauchi R (2012) Genome sequencing reveals agronomically important loci in rice using MutMap. *Nat Biotechnol* 30:174–178
- Blankenberg D, Von Kuster G, Coraor N, Ananda G, Lazarus R, Mangano M, Nekrutenko A, Taylor J (2010) Galaxy: a web-based genome analysis tool for experimentalists. In: *Current protocols in molecular biology*, Chap 19.10, vol 89, pp 19.10.1–19.10.21
- Bolger AM, Lohse M, Usadel B (2014) Trimmomatic: a flexible trimmer for Illumina sequence data. *Bioinformatics* 30:2114–2120
- Bradbury PJ, Zhang Z, Kroon DE, Casstevens TM, Ramdoss Y, Buckler ES (2007) TASSEL: software for association mapping of complex traits in diverse samples. *Bioinformatics* 23:2633–2635
- Davey JW, Hohenlohe PA, Etter PD, Boone JQ, Catchen JM, Blaxter ML (2011) Genome-wide genetic marker discovery and genotyping using next-generation sequencing. *Nat Rev Genet* 12:499–510
- Gaut BS (2002) Evolutionary dynamics of grass genomes. *New Phytol* 154:15–28
- Giardine B, Riemer C, Hardison RC, Burhans R, Elnitski L, Shah P, Zhang Y, Blankenberg D, Albert I, Taylor J, Miller W, Kent WJ, Nekrutenko A (2005) Galaxy: a platform for interactive large-scale genome analysis. *Genome Res* 15:1451–1455
- Goecks J, Nekrutenko A, Taylor J (2010) Galaxy: a comprehensive approach for supporting accessible, reproducible, and transparent computational research in the life sciences. *Genome Biol* 11:R86
- Grabherr MG, Haas BJ, Yassour M, Levin JZ, Thompson DA, Amit I, Adiconis X, Fan L, Raychowdhury R, Zeng Q, Chen Z, Mauceli E, Hacohen N, Gnirke A, Rhind N, di Palma F, Birren BW, Nusbaum C, Lindblad-Toh K, Friedman N, Regev A (2011) Full-length transcriptome assembly from RNA-Seq data without a reference genome. *Nat Biotechnol* 29:644–652
- Haas BJ, Papanicolaou A, Yassour M, Grabherr M, Blood PD, Bowden J, Couger MB, Eccles D, Li B, Lieber M, Macmanes MD, Ott M, Orvis J, Pochet N, Strozzi F, Weeks N, Westerman R, Williams T, Dewey CN, Henschel R, Leduc RD, Friedman N, Regev A (2013) De novo transcript sequence reconstruction from RNA-seq using the Trinity platform for reference generation and analysis. *Nat Protoc* 8:1494–1512
- Iehisa JCM, Shimizu A, Sato K, Nasuda S, Takumi S (2012) Discovery of high-confidence single nucleotide polymorphisms from large-scale de novo analysis of leaf transcripts of *Aegilops tauschii*, a wild wheat progenitor. *DNA Res* 19:487–497
- Iehisa JCM, Shimizu A, Sato K, Nishijima R, Sakaguchi K, Matsumoto T, Tanaka T, Sakai H, Amano N, Kanamori H, Kurita K, Kikuta A, Kamiya K, Yamamoto M, Ikawa H, Fujii N, Hori K, Itoh T, Sato K (2011) Comprehensive sequence analysis of 24,783 barley full-length cDNAs derived from 12 clone libraries. *Plant Physiol* 156:20–28
- Matsuoka Y, Nasuda S, Ashida Y, Nitta M, Tsujimoto H, Takumi S, Kawahara T (2013) Genetic basis for spontaneous hybrid genome doubling during allopolyploid speciation of common wheat shown by natural variation analyses of the paternal species. *PLoS One* 8:e68310
- Matsuoka Y, Takumi S, Kawahara T (2015) Intraspecific lineage divergence and its association with reproductive trait change during species range expansion in central Eurasian wild wheat *Aegilops tauschii* Coss. (Poaceae). *BMC Evol Biol* 15:213
- Mayer KFX, Martis M, Hedley PE, Šimková H, Liu H, Morris JA, Steuernagel B, Taudien S, Roessner S, Gundlach H, Kubaláková M, Suchánková P, Murat F, Felder M, Nussbaumer T, Graner A, Salse J, Endo T, Sakai H, Tanaka T, Itoh T, Sato K, Platzer M, Matsumoto T, Scholz U, Doležel J, Waugh R, Stein N (2011) Unlocking the barley genome by chromosomal and comparative genomics. *Plant Cell* 23:1249–1263
- development for the wheat D genome based on single nucleotide polymorphisms identified from transcripts in the wild wheat progenitor *Aegilops tauschii*. *Theor Appl Genet* 127:261–271
- International Barley Genome Sequencing Consortium (2012) A physical, genetic and functional sequence assembly of the barley genome. *Nature* 491:711–716
- Jia J, Zhao S, Kong X, Li Y, Zhao G, He W, Appels R, Pfeifer M, Tao Y, Zhang X, Jing R, Zhang C, Ma Y, Gao L, Gao C, Spannagl M, Mayer KFX, Li D, Pan S, Zheng F, Hu Q, Xia X, Li J, Liang Q, Chen J, Wicker T, Gou C, Kuang H, He G, Luo Y, Keller B, Xia Q, Lu P, Wang J, Zou H, Zhang R, Xu J, Gao J, Middleton C, Quan Z, Liu G, Wang J, International Wheat Genome Sequencing Consortium, Yang H, Liu X, He Z, Mao L, Wang J (2013) *Aegilops tauschii* draft genome sequence reveals a gene repertoire for wheat adaptation. *Nature* 496:91–95
- Kersey PJ, Allen JE, Armean I, Boddu S, Bolt BJ, Carvalho-Silva D, Christensen M, Davis P, Falin LJ, Grabmueller C, Humphrey J, Kerhornou A, Khobova J, Aranganathan NK, Langridge N, Lowy E, McDowall MD, Maheswari U, Nuhn M, Ong CK, Overduin B, Paulini M, Pedro H, Perry E, Spudich G, Tapanari E, Walts B, Williams G, Tello-Ruiz M, Stein J, Wei S, Ware D, Bolser DM, Howe KL, Kulesha E, Lawson D, Maslen G, Staines DM (2015) Ensembl genomes 2016: more genomes, more complexity. *Nucleic Acids Res* 44:574–580
- Kosugi S, Natsume S, Yoshida K, MacLean D, Cano L, Kamoun S, Terauchi R (2013) Coval: improving alignment quality and variant calling accuracy for next-generation sequencing data. *PLoS One* 8:e75402
- Kumar S, Banks TW, Cloutier S (2012) SNP discovery through next-generation sequencing and its applications. *Int J Plant Genomics*. doi:10.1155/2012/831460
- Langmead B, Salzberg SL (2012) Fast gapped-read alignment with Bowtie 2. *Nat Methods* 9:357–359
- Li H, Handsaker B, Wysoker A, Fennell T, Ruan J, Homer N, Marth G, Abecasis G, Durbin R, Subgroup 1000 Genome Project Data Processing (2009) The sequence alignment/map format and SAMtools. *Bioinformatics* 25:2078–2079
- Luo M-C, Gu YQ, You FM, Deal KR, Ma Y, Hu Y, Huo N, Wang Y, Wang J, Chen S, Jorgensen CM, Zhang Y, McGuire PE, Pasternak S, Stein JC, Ware D, Kramer M, McCombie WR, Kianian SF, Martis MM, Mayer KFX, Sehgal SK, Li W, Gill BS, Bevan MW, Šimková H, Doležel J, Weining S, Lazo GR, Anderson OD, Dvorak J (2013) A 4-gigabase physical map unlocks the structure and evolution of the complex genome of *Aegilops tauschii*, the wheat D-genome progenitor. *Proc Natl Acad Sci USA* 110:7940–7945

- Mizuno N, Yamasaki M, Matsuoka Y, Kawahara T, Takumi S (2010) Population structure of wild wheat D-genome progenitor *Aegilops tauschii* Coss.: implications for intraspecific lineage diversification and evolution of common wheat. *Mol Ecol* 19:999–1013
- Nishijima R, Iehisa JCM, Matsuoka Y, Takumi S (2014) The cuticular wax inhibitor locus *Iw2* in wild diploid wheat *Aegilops tauschii*: phenotypic survey, genetic analysis, and implications for the evolution of common wheat. *BMC Plant Biol* 14:246
- Quinlan AR, Hall IM (2010) BEDTools: a flexible suite of utilities for comparing genomic features. *Bioinformatics* 26:841–842
- Sehgal D, Vikram P, Sansaloni CP, Ortiz C, Saint Pierre C, Payne T, Ellis M, Amri A, Petroli CD, Wenzl P, Singh S (2015) Exploring and mobilizing the gene bank biodiversity for wheat improvement. *PLoS One* 10:e0132112
- Takagi H, Uemura A, Yaegashi H, Tamiru M, Abe A, Mitsuoka C, Utsushi H, Natsume S, Kanzaki H, Matsumura H, Saitoh H, Cano LM, Kamoun S, Terauchi R (2013) Methods MutMap-Gap: whole-genome resequencing of mutant F2 progeny bulk combined with *de novo* assembly of gap regions identifies the rice blast resistance gene *Pii*. *New Phytol* 200:276–283
- Takumi S, Koyama K, Fujiwara K, Kobayashi F (2011) Identification of a large deletion in the first intron of the *Vrn-D1* locus, associated with loss of vernalization requirement in wild wheat progenitor *Aegilops tauschii* Coss. *Genes Genet Syst* 86:183–195
- Tsunewaki K (1966) Comparative gene analysis of common wheat and its ancestral species. II. Waxiness, growth habit and awnedness. *Jpn J Bot* 19:175–229
- Townsley BT, Covington MF, Ichihashi Y, Zumstein K, Sinha NR (2015) BrAD-seq: Breath Adapter Directional sequencing: a streamlined, ultra-simple and fast library preparation protocol for strand specific mRNA library construction. *Front Plant Sci* 6:366
- Wicker T, Mayer KFX, Gundlach H, Martis M, Steuernagel B, Scholz U, Šimková H, Kubaláková M, Choulet F, Taudien S, Platzer M, Feuillet C, Fahima T, Budak H, Dolezel J, Keller B, Stein N (2011) Frequent gene movement and pseudogene evolution is common to the large and complex genomes of wheat, barley, and their relatives. *Plant Cell* 23:1706–1718
- Wu TD, Watanabe CK (2005) GMAP: a genomic mapping and alignment program for mRNA and EST sequences. *Bioinformatics* 21:1859–1875
- Yang C, Zhao L, Zhang H, Yang Z, Wang H, Wen S, Zhang C, Rustgi S, von Wettstein D, Liu B (2014) Evolution of physiological responses to salt stress in hexaploid wheat. *Proc Natl Acad Sci* 111:11882–11887
- Zhang J, Kobert K, Flouri T, Stamatakis A (2014) PEAR: a fast and accurate Illumina Paired-End reAd mergeR. *Bioinformatics* 30:614–620